Self-consistent four-point closure for transport in steady random flows

Marco Dentz*
Department of Geotechnical Engineering and Geosciences, Technical University of Catalonia (UPC), Barcelona, Spain

Daniel M. Tartakovsky†
Department of Mechanical & Aerospace Engineering, University of California San Diego, La Jolla, California 92093, USA

(Received 29 August 2007; revised manuscript received 21 February 2008; published 17 June 2008)

Ensemble averaging of advection-dispersion equations describing transport of a passive scalar in incompressible random velocity fields requires a closure approximation. Commonly used approaches, such as the direct interaction approximation and large-eddy simulations as well as equivalent renormalization schemes, employ so-called two-point (or one-loop) closures. These approaches have proven to be adequate for transport in zero-mean (unbiased) time-dependent random velocity fields with increasing accuracy for decreasing temporal coherence. In the opposite limit of steady velocity fields with finite bias, however, these schemes fail to predict effective transport properties both quantitatively and qualitatively, leading to an obvious inconsistency for transverse dispersion in two spatial dimensions. For this case, two-point closures predict that macroscopic transverse dispersion increases as the square root of the disorder variance while it has been proven rigorously that there is no disorder-induced contribution to macroscopic transverse dispersion for purely advective transport. Furthermore, two-point closures significantly underestimate the disorder-induced contribution to longitudinal dispersion. We derive a four-point closure for stochastically averaged transport equations that goes beyond classical one-loop schemes and demonstrate that it is exact for transverse dispersion and correctly predicts an increase of the longitudinal disorder-induced dispersion coefficient with the square of the variance of the strong disorder. The predicted values of asymptotic longitudinal dispersion coefficients are consistent with those obtained via Monte Carlo random walk simulations.

DOI: 10.1103/PhysRevE.77.066307 PACS number(s): 47.27.tb, 05.60.−k, 92.40.Kf, 02.50.Ey

I. INTRODUCTION

We study transport of a passive scalar in steady incompressible Gaussian random flow fields with nonzero mean velocity (bias). Transport of passive scalars in flow fields varying randomly in space has been investigated in the past as a steady-state limit of turbulent transport (the so-called frozen turbulence) (e.g., [2–6]), as an approximation for solute transport in random porous media (e.g., [7–12]), and as a tool to analyze random walks in random environments (e.g., [7,13–16]).

Most analyses of Gaussian flow models (e.g., [2–4,14–17]) dealt with zero-mean (unbiased) velocity fields, often stipulating that incorporation of the bias is straightforward. In various applications, including transport in porous media, the mean flow velocity is nonzero. Analytical and numerical analyses of such flows showed that the addition of a bias is nontrivial and leads to a qualitatively and quantitatively different transport behavior (e.g., [13]). Gaussian random flow models with nonzero bias have been used to study fundamental transport properties in two- and three-dimensional heterogeneous porous media (e.g., [9–12,18–21]).

The combined effect of local diffusion, microdispersion, and velocity fluctuations is to increase the spreading of a passive scalar in a spatially random velocity field. An accurate quantification of the impact of spatial fluctuations on the dispersion of a passive scalar is of paramount importance for characterization of transport in heterogeneous environments. Disorder-induced macrodispersion coefficients can be orders of magnitude larger than their local or microscale counterparts. The qualitative and quantitative understanding of heterogeneity-induced contaminant spreading has been the subject of extensive research in groundwater hydrology (e.g., [22,23]).

Asymptotic disorder-induced spreading can be characterized by macrodispersion coefficients. Within a stochastic framework, these are often defined by the temporal rate of change of the second centered moments of the ensemble averaged (normalized) particle distribution $\bar{c}(\mathbf{x},t)$ (e.g., [24,25]),

$$D_{ij} = \frac{1}{2}\frac{d}{dt}\left(\int d\mathbf{x}\, x_i x_j \bar{c}(\mathbf{x},t) - \int d\mathbf{x}\, x_i \bar{c}(\mathbf{x},t) \int d\mathbf{x}\, x_j \bar{c}(\mathbf{x},t) \right) - D_{ij}^m, \tag{1}$$

where D_{ij}^m $(i,j,=1,\ldots,d)$ are the microdispersion coefficients in d spatial dimensions.

Analyses of transport in heterogeneous environments routinely employ perturbation expansions in the variance of velocity fluctuations. Lowest-order perturbation expansions predict a macroscopic disorder-induced contribution to the long-time asymptotic values of the longitudinal (in the direction of the mean flow) dispersion coefficient, while the contributions to the transverse dispersion coefficient scale with the microdispersion coefficient, which means they vanish in the limiting case of zero local dispersion. Higher-order perturbative closures have been used, e.g., [26–29], to study the

*marco.dentz@upc.edu
†dmt@ucsd.edu

impact of higher-order terms. Specifically, higher-order corrections to the transverse macrodispersion coefficient have been derived in [26,27] by employing a Lagrangian framework and neglecting local dispersion. As time $t \to \infty$, these contributions tend to 0, in agreement with the leading-order approximations, nonperturbative numerical simulations [21,30], and a nonperturbative exact analysis [1] of transport in two-dimensional incompressible random flow.

Perturbation approaches break down as disorder increases, which occurs when transport takes place in strongly heterogeneous porous media. Renormalization theory (e.g., [10,31–35]), multiscale homogenization methods (e.g., [35–38]), and self-consistent closures (e.g., [26,39–44]) are some of the most often used alternatives (see also the review [34] and the references therein). Unlike perturbative closures (e.g., [28,29,43]), these methods represent (partial) resummation schemes of the perturbation series which take into account certain classes of contributions at every approximation order (and thus an infinite number of higher-order terms), while other contributions are disregarded.

The direct interaction approximation (DIA), which relies on a two-point closure of the underlying transport problem (e.g., [39,40]), is an example of self-consistent closures. The exactly solvable problem of transport in unbiased shear flow with fluctuating cross sweep is used in [43] to compare the performance of the DIA with that of second-order perturbation closures, their local counterparts, and renormalized Lagrangian approaches. While the DIA gives satisfying results for the dispersion of a scalar in turbulent flow (e.g., [2,40,43,44]), it fails to adequately describe macrodispersion in two-dimensional biased random flows. In fact, as pointed out by Kraichnan and others (e.g., [2,44]), the DIA is exact for a random velocity field that is δ correlated in time. Here, however, we deal with the opposite limit of frozen or quenched disorder.

Classical renormalization group studies of turbulence (or more appropriately, properties of randomly stirred fluids) (e.g., [45–47]) employ schemes that are equivalent to the two-point closures. They result in the so-called one-loop resummation schemes for the eddy diffusivity (in the context of the present paper termed macrodispersion) resulting from the DIA scheme [44].

However, the DIA and equivalent two-point closure approximations fail to describe the correct behavior of the transverse dispersion coefficient in two dimensions, and predict a macroscopic disorder-induced contribution that scales with the square root of the disorder variance. Moreover, numerical simulations [12,21,30] of transport in steady two- and three-dimensional Gaussian random flow fields show that the DIA underestimates the longitudinal macrodispersion coefficients. In three dimensions, the DIA closure captures a macroscopic contribution to transverse dispersion but significantly underestimates its value. We show that this systemic failure stems from the omission of a certain class of higher-order terms.

In this paper, we derive a four-point closure scheme that takes these contributions into account and goes beyond the two-point closures routinely employed in the literature. This four-point closure is exact for the transverse dispersion coefficient in two dimensions and is consistent with Monte Carlo simulations for the longitudinal dispersion coefficient. The developed closure overcomes the limitations of commonly used two-point closure schemes, such as the DIA and one-loop renormalization approaches.

II. BASICS

A. Transport model

The time evolution of a scalar field $c(\mathbf{x},t)$ in a spatially random flow field $\mathbf{u}(\mathbf{x})$ is described by

$$\frac{\partial c(\mathbf{x},t)}{\partial t} + \mathbf{u}(\mathbf{x}) \cdot \nabla c(\mathbf{x},t) - \nabla \cdot \mathbf{D}^m \nabla c(\mathbf{x},t) = 0, \tag{2}$$

where $\mathbf{D}^m$ is the microdispersion tensor. The random flow velocity $\mathbf{u}(\mathbf{x})$ is divergence-free, $\nabla \cdot \mathbf{u}(\mathbf{x}) = 0$. The initial distribution is given by $c(\mathbf{x},0) = \delta(\mathbf{x})$. Let $G(\mathbf{x},t|\mathbf{x}',t')$ denote the Green's function associated with Eq. (2). Its initial distribution is given by

$$G(\mathbf{x},t'|\mathbf{x}',t') = \delta(\mathbf{x}-\mathbf{x}'). \tag{3}$$

The elementary properties of Green's functions suggest that

$$G(\mathbf{x},t|\mathbf{x}',t') \equiv g(\mathbf{x},t-t'|\mathbf{x}') \tag{4}$$

and that the scalar field $c(\mathbf{x},t)$ is given in terms of the Green's function by

$$c(\mathbf{x},t) = g(\mathbf{x},t|\mathbf{0}). \tag{5}$$

B. Stochastic model

We assume that the random flow field $\mathbf{u}(\mathbf{x})$ is statistically homogeneous (stationary), i.e., that its (functional) distribution $\mathcal{P}\{\mathbf{u}(\mathbf{x})\}$ satisfies

$$\mathcal{P}\{\mathbf{u}(\mathbf{x})\} = \mathcal{P}\{\mathbf{u}(\mathbf{x}+\mathbf{L})\}, \tag{6}$$

where $\mathbf{L}$ is an arbitrary constant vector. Statistical homogeneity implies that the ensemble mean velocity $\bar{\mathbf{u}}$ is independent of the position $\mathbf{x}$. We use Reynolds' decomposition to represent $\mathbf{u}$ as the sum of its (constant) mean $\bar{\mathbf{u}}$ and random zero-mean fluctuations $\mathbf{u}'(\mathbf{x})$ about it,

$$\mathbf{u}(\mathbf{x}) = \bar{u}\mathbf{e}_1 + \mathbf{u}'(\mathbf{x}), \tag{7}$$

where $\mathbf{e}_1$ is the unit vector of a coordinate system aligned with the direction of mean flow. Furthermore, spatial homogeneity implies that two-point covariance functions of $u_i'(\mathbf{x})$ are given by

$$\overline{u_i'(\mathbf{x})u_j'(\mathbf{x}')} \equiv \sigma^2 C_{ij}(\mathbf{x}-\mathbf{x}'), \tag{8}$$

where σ^2 and $C_{ij}(\mathbf{x})$ are the (constant) variance and correlation function, respectively.

Finally, the statistical homogeneity of $\mathbf{u}(\mathbf{x})$ implies (see Appendix B) the equivalence between the ensemble mean Green's function $\overline{g(\mathbf{x},t|\mathbf{x}')}$ and the ensemble mean scalar field $\bar{c}(\mathbf{x}-\mathbf{x}',t)$,

$$\overline{g(\mathbf{x},t|\mathbf{x}')} = \bar{c}(\mathbf{x}-\mathbf{x}',t). \tag{9}$$

Thus, in the following we use the terms propagator and concentration for the Green's function as well as for the scalar field $c(\mathbf{x},t)$.

Lengths are now rescaled according to $x_i=\hat{x}_i l$ with l a typical length scale; times are rescaled according to $t=\hat{t}\tau_u$ where $\tau_u=l/\bar{u}$ is a characteristic advection time scale. The random flow field is nondimensionalized according to $\mathbf{u}(\mathbf{x})=\hat{\mathbf{u}}(\mathbf{x})\bar{u}$, its variance as $\sigma^2=\hat{\sigma}^2\bar{u}^2$, and the microdispersion tensor as $\mathbf{D}^m=\hat{D}^m/(l\bar{u})$. To simplify the notation, in the following we drop the carets that denote nondimensional quantities.

Substituting Eq. (7) into Eq. (2) leads to an integral equation in the Fourier-Laplace space (Appendix A)

$$\tilde{c}^*(\mathbf{k},s)=\tilde{c}_0^*(\mathbf{k},s)+\tilde{c}_0^*(\mathbf{k},s)\int_{\mathbf{k}'} i\mathbf{k}\cdot\tilde{\mathbf{u}}'(\mathbf{k}')\tilde{c}^*(\mathbf{k}-\mathbf{k}',s). \tag{10}$$

Here $\tilde{c}_0^*(\mathbf{k},s)$ is the Fourier-Laplace transform of the "bare" propagator $c_0(\mathbf{x},t)$ that is given by

$$\tilde{c}_0^*(\mathbf{k},s)=(s-ik_1+\mathbf{k}\cdot\mathbf{D}^m\mathbf{k})^{-1} \tag{11}$$

and

$$\int_{\mathbf{k}}\cdots\equiv\int\frac{d\mathbf{k}}{(2\pi)^d}\cdots. \tag{12}$$

Following the standard procedure (e.g., [48]), the ensemble average of Eqs. (10) and (11) can be written in the form of the Dyson equation for the mean $\bar{c}(\mathbf{x},t)$,

$$\bar{\tilde{c}}^*(\mathbf{k},s)=[s-ik_1+\mathbf{k}\cdot\mathbf{D}^m\mathbf{k}-\Sigma(\mathbf{k},s)]^{-1}. \tag{13}$$

The as yet unknown function $\Sigma(\mathbf{k},s)$ is analogous to the self-energy in quantum theory [36]. In the present context, $\Sigma(\mathbf{k},s)$ is known as the generalized diffusivity [2,36]. The physical meaning of $\Sigma(\mathbf{k},s)$ becomes apparent if one substitutes the average concentration $\bar{\tilde{c}}^*(\mathbf{k},s)$ in Eq. (13) into the Laplace transform of the macrodispersion coefficients in Eq. (1),

$$D_{ij}^*(s)=-s^{-1}\left.\frac{\partial^2\Sigma(\mathbf{k},s)}{\partial k_i\,\partial k_j}\right|_{\mathbf{k}=\mathbf{0}}. \tag{14}$$

To obtain an operational expression for $\Sigma(\mathbf{k},s)$, we note that in the long-time limit the dispersion coefficients $D_{ij}(t)$ reach their (as yet unknown) asymptotic values D_{ij}^a,

$$D_{ij}^a=\lim_{t\to\infty}D_{ij}(t)=\lim_{s\to 0}sD_{ij}^*(s). \tag{15}$$

For large distances and long times, or equivalently, small wave numbers and frequencies, the generalized diffusivity can be approximated by (e.g., [36,49])

$$\Sigma(\mathbf{k},0)\approx-\mathbf{k}\cdot\mathbf{D}^a\mathbf{k}. \tag{16}$$

Thus, the average concentration (13) is asymptotically given by

$$\bar{\tilde{c}}^*(\mathbf{k},s)=(s-ik_1+\mathbf{k}\cdot\mathbf{D}^m\mathbf{k}+\mathbf{k}\cdot\mathbf{D}^a\mathbf{k})^{-1}. \tag{17}$$

Equation (13) yields a formal (nondimensional) effective equation for the average concentration (e.g., [32,40,50,51]),

$$s\bar{\tilde{c}}^*(\mathbf{k},s)-ik_1\bar{\tilde{c}}^*(\mathbf{k},s)+\mathbf{k}\cdot\mathbf{D}^m\mathbf{k}\bar{\tilde{c}}^*(\mathbf{k},s)-\Sigma(\mathbf{k},s)\bar{\tilde{c}}^*(\mathbf{k},s)=1, \tag{18}$$

which is equivalent to the Dyson equation. Such a formal effective equation can also be derived within the Zwanzig-Mori projector formalism [35,43,52,53]. Since $\Sigma(\mathbf{k},s)$ depends on the unknown mixed moments of the random fluctuations of the flow field and the full propagator, these equations are incomplete and require a closure approximation. In the next section, we briefly review well-known second- and fourth-order perturbative closures. For strongly heterogeneous random flows, however, such low-order perturbation closures are not sufficient (e.g., [32,50]).

C. Perturbation theory

To make the presentation more compact, we employ a diagrammatic representation (e.g., [36,54]) of integral expressions; see also the recent textbook by Sadovskii [55]. The full propagator $\tilde{c}^*(\mathbf{k},s)$ is represented by a horizontal double line, the bare propagator $\tilde{c}_0^*(\mathbf{k},s)$ by a single horizonal line, and the random perturbation $\mathbf{u}'(\mathbf{k}')$ by a single vertical line. The intersection of the horizontal and vertical lines defines a vertex, which is associated with the factor $i(\mathbf{k}-\mathbf{k}')/(2\pi)^d$. The latter is contracted with $\mathbf{u}'(\mathbf{k}')$. The wave vectors $\mathbf{k}$ sum up from the right to the left to the value on the left. Thus, the wave vectors are determined uniquely by the one on the left. The inner wave vectors, i.e., the vectors associated with $\mathbf{u}'(\mathbf{k})$, in a diagram are integrated over. Thus, the integral Eq. (10) can be represented by

(19)

Equation (19) can be iterated into a perturbation series in terms of the velocity fluctuations. Truncating this series at fourth order, we obtain

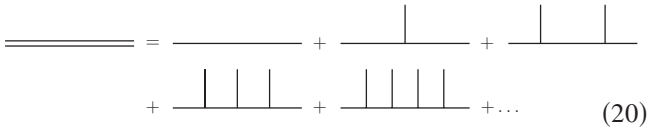

(20)

If the random velocity field $\tilde{\mathbf{u}}'(\mathbf{k})$ is Gaussian, all $(2n)$-point correlation functions can be expressed in terms of the two-point correlation

$$\overline{\tilde{u}_i'(\mathbf{k})\tilde{u}_j'(\mathbf{k}')}=(2\pi)^d\delta(\mathbf{k}+\mathbf{k}')\tilde{C}_{ij}(\mathbf{k}), \tag{21}$$

and all $(2n-1)$-point correlation functions vanish. Thus, the ensemble average is performed diagrammatically by pairwise connection of vertices. The sum of the wave vectors at a vertex, where wave vectors of outgoing lines are subtracted, is zero. According to Wick's theorem (e.g., [48]), all possible combinations of pairs of vertices have to be summed up at a given approximation order. The average over a diagram with an odd number of vertices is zero. Two connected vertices are associated with the correlation matrix $\tilde{\mathbf{C}}(\mathbf{k})$. This matrix is contracted with the wave vectors of the

ingoing and outgoing horizontal lines and multiplied by a factor $-(2\pi)^{-d}$. The inner wave vectors are integrated over.

In the diagrammatic notation, the fourth-order expansion of $\overline{\tilde{c}^*}(\mathbf{k},s)$ is obtained by averaging Eq. (20) which leads to

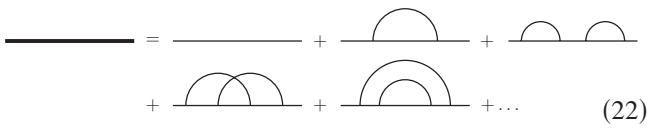

(22)

and the Dyson equation (18) as

(23)

Here the ensemble-averaged concentration is represented by the bold line, and the circle denotes the generalized diffusivity $\Sigma(\mathbf{k},s)$. Using the series expansion for the average concentration and relation (13), one obtains a series expansion for $\Sigma(\mathbf{k},s)$. Up to sixth order it is given by

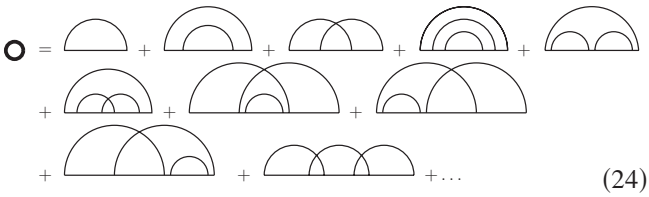

(24)

The generalized diffusivity is the sum of all irreducible diagrams, i.e., the diagrams that cannot be decomposed in two by cutting a single internal line (e.g., [36]).

Substituting Eq. (24) into Eq. (14), we obtain an expression for the macrodispersion coefficients,

$$D_{ij}(t) = D_{ij}^m + \sum_{n=1}^{\infty} \delta^{(n)} D_{ij}(t), \tag{25}$$

where $\delta^{(n)}D_{ij}(t)$ are defined in terms of the diagrams contributing to the generalized diffusivity at every approximation order. Under some conditions, such infinite series can be computed analytically, as was done in [56] for transport in one-dimensional random environments. Under more general conditions, these series have to truncated or approximated by partial summations obtained through closure schemes. In the following, we briefly review the second- and fourth-order perturbation approximations of the macrodispersion coefficients.

1. Second-order approximation

The second-order approximations of the longitudinal, $D_{11}(t)$, and transverse, $D_{22}(t)$, macrodispersion coefficients are given by the one-loop diagram in Eq. (24) (e.g., [24,25,57]),

$$\delta^{(2)} D_{ij}(t) = \int_0^t dt' \int_{\mathbf{k}'} \tilde{c}_0(-\mathbf{k}',t') \tilde{C}_{ij}(\mathbf{k}'), \tag{26}$$

where $i=1,\ldots,d$. The off-diagonal dispersion coefficients are zero for symmetry reasons. For a short-range correlation function, one obtains in $d=2$ dimensions in the limit of $\mathbf{D}^m \to \mathbf{0}$,

$$\delta^{(2)} D_{11}^a \propto \sigma^2, \quad \delta^{(2)} D_{22}^a = 0, \quad t \to \infty. \tag{27}$$

Note that, as pointed out by many authors (e.g., [24,25,57]), the second-order approximation yields no macroscopic contribution to the transverse dispersion coefficient.

2. Fourth-order approximation

The fourth-order contribution to the macrodispersion coefficient is given by the loop and cross diagrams in Eq. (24) (e.g., [26,27]),

$$\delta^{(4)} D_{ij}(t) = \delta^{(4,l)} D_{ij}(t) + \delta^{(4,c)} D_{ij}(t), \tag{28a}$$

where the superscripts (l) and (c) denote the double-loop and cross contributions, respectively. These are given by

$$\delta^{(4,l)} D_{ij}(t) = -\sigma^4 \int_{\mathbf{k}'} \int_{\mathbf{k}''} \tilde{c}_0^*(-\mathbf{k}',s) \overline{\tilde{c}^*}(-\mathbf{k}'-\mathbf{k}'',s) \times \tilde{c}_0^*(-\mathbf{k}',s) \tilde{C}_{ij}(\mathbf{k}') \mathbf{k}' \cdot \tilde{\mathbf{C}}(\mathbf{k}'') \mathbf{k}' \tag{28b}$$

and

$$\delta^{(4,c)} D_{ij}(t) = -\sigma^4 \int_{\mathbf{k}'} \int_{\mathbf{k}''} \tilde{c}_0^*(-\mathbf{k}',s) \overline{\tilde{c}^*}(-\mathbf{k}'-\mathbf{k}'',s) \times \tilde{c}_0^*(-\mathbf{k}'',s) \tilde{C}_{il}(\mathbf{k}') k_l'' k_m' \tilde{C}_{mj}(\mathbf{k}''), \tag{28c}$$

where the summation is carried out over repeated indices. In two spatial dimensions, taking the limit of Eq. (28) as $\mathbf{D}^m \to \mathbf{0}$ yields

$$\delta^{(4)} D_{11}^a \propto \sigma^4, \quad \delta^{(4)} D_{22}^a = 0, \quad t \to \infty. \tag{29}$$

The transverse dispersion coefficient is zero in fourth order because the loop and cross diagrams cancel each other. Clearly, this mechanism is not represented in a one-loop self-consistent resummation scheme as detailed in the following.

III. SOME EXACT RELATIONS

The stationarity of the random flow field implies that the ensemble average of Eq. (10) can be written as (see Appendix C)

$$\overline{\tilde{c}^*}(\mathbf{k},s) = \tilde{c}_0^*(\mathbf{k},s) + \tilde{c}_0^*(\mathbf{k},s)^2 \mathbf{k} \cdot \boldsymbol{\phi}(\mathbf{k},s) \mathbf{k}, \tag{30a}$$

where

$$\boldsymbol{\phi}(\mathbf{k},s) = -\int_{\mathbf{k}'} \int_{\mathbf{k}''} \overline{\tilde{\mathbf{u}}'(\mathbf{k}') \otimes \tilde{\mathbf{u}}'(\mathbf{k}'') \tilde{c}^*(\mathbf{k}-\mathbf{k}',s)} \tag{30b}$$

and $\otimes$ denotes the tensor product. Comparison of Eq. (13) and (30) yields

$$\Sigma(\mathbf{k},s) = \mathbf{k} \cdot \left[\boldsymbol{\phi}(\mathbf{k},s) - \frac{\tilde{c}_0^*(\mathbf{k},s) \boldsymbol{\phi}(\mathbf{k},s) \mathbf{k} \otimes \mathbf{k} \boldsymbol{\phi}(\mathbf{k},s)}{1 + \tilde{c}_0^*(\mathbf{k},s) \mathbf{k} \cdot \boldsymbol{\phi}(\mathbf{k},s) \mathbf{k}} \right] \mathbf{k}, \tag{31}$$

which demonstrates without any recourse to perturbation theory that $\Sigma(\mathbf{k},s) = \mathbf{k} \cdot \boldsymbol{\varphi}(\mathbf{k},s) \mathbf{k}$, with $\boldsymbol{\varphi}(\mathbf{k},s)$ given by the expression in large parentheses in Eq. (31).

Substituting Eq. (31) into Eq. (14) gives for the macrodispersion coefficient

$$D_{ij}^{*}(s) = -s^{-1}\phi_{ij}(\mathbf{0},s). \tag{32}$$

The asymptotic long-time behavior ($s \to 0$) of the macrodispersion coefficients is given by

$$D_{ij}^{a} = -\phi_{ij}(\mathbf{0},0). \tag{33}$$

Taking the inverse Laplace transform of Eq. (30b) and (32) leads to

$$D_{ij}(t) = D_{ij}^{m} + \int_0^t d\tau \int_{\mathbf{k}'} \int_{\mathbf{k}''} \overline{\tilde{u}_i'(\mathbf{k}')\tilde{u}_j'(\mathbf{k}'')\tilde{c}(-\mathbf{k}',t')}. \tag{34}$$

Substituting the Green's function $\tilde{g}(\mathbf{q},t|\mathbf{k})$ into Eq. (34) yields

$$D_{ij}(t) = D_{ij}^{m} + \int_0^t dt' \int_{\mathbf{q}} \int_{\mathbf{k}'} \overline{\tilde{u}_i'(\mathbf{k}')\tilde{\chi}_j(\mathbf{q},t')}, \tag{35a}$$

where $\tilde{\chi}_j(\mathbf{k},t)$ is the Fourier transform of the auxiliary function (e.g., [35,58])

$$\chi_j(\mathbf{x},t) = \int d\mathbf{x}' u_j'(\mathbf{x}') c(\mathbf{x},t|\mathbf{x}'). \tag{35b}$$

This function is defined as a solution of the advection-dispersion equation (2) subject to the initial condition

$$\chi_j(\mathbf{x},t=0) = u_j'(\mathbf{x}). \tag{36}$$

Representations of the macrodispersion coefficient $D_{ij}(t)$ in terms of the auxiliary function $\tilde{\chi}_j(\mathbf{x},t)$ similar to Eq. (35) were derived and analyzed previously with homogenization approaches (e.g., [1,34,35,38,58–61]). For the asymptotic ($t \to \infty$) macrodispersion coefficients, we obtain

$$D_{ij}^{a} = D_{ij}^{m} + \int_{\mathbf{q}} \int_{\mathbf{k}'} \overline{\tilde{u}_i'(\mathbf{k}')\tilde{\chi}_j^{*}(\mathbf{q},0)}. \tag{37}$$

In $d=2$ spatial dimensions and for vanishing microdispersion ($\mathbf{D}^m \to \mathbf{0}$), the exact solution for $\tilde{\chi}_2^{*}(\mathbf{q},0)$ is [1]

$$\tilde{\chi}_2^{*}(\mathbf{q},0) = \frac{\tilde{u}_2'(\mathbf{q})}{ik_1}, \tag{38}$$

as can be checked by inspection. Substituting Eq. (38) into Eq. (37) with $i=2$ yields an exact expression for the transverse dispersion coefficient, which is identical to the long-time limit of the second-order perturbation theory expression (26). Thus, we obtain as an exact result that there is no macroscopic contribution to transverse dispersion. This has been proved in [1] in the framework of a homogenization theory approach.

IV. CLOSURES, SELF-CONSISTENCY, AND RESUMMATION

For transport in strongly heterogeneous flow fields, low-order perturbation approaches are not sufficient. Here we review the direct interaction approximation as a self-consistent one-loop resummation scheme and discuss its failure in $d=2$ dimensions. Then we develop a higher-order closure scheme that overcomes the inconsistency inherent in the DIA.

The transport problem is closed in terms of the function $\boldsymbol{\phi}(\mathbf{k},s)$ defined by Eq. (30b). An expansion for $\boldsymbol{\phi}(\mathbf{k},s)$ is obtained by inserting Eq. (22) into Eq. (30b). This yields up to fourth order,

(39)

where the rectangle denotes $\mathbf{k}\cdot\boldsymbol{\phi}(\mathbf{k},s)\mathbf{k}$. Expanding (31) in terms of $\boldsymbol{\phi}(\mathbf{k},s)$ in (39) yields a closure for the generalized diffusivity $\Sigma(\mathbf{k},s)$,

(40)

The self-consistency condition is imposed by the fact that only irreducible diagrams can contribute to the generalized diffusivity. In the following we briefly summarize the derivation of the DIA and elucidate its meaning as a resummation scheme of the perturbation series in order to contrast it with a different four-point closure.

A. Direct interaction approximation

The DIA (e.g., [49,50]) is obtained by breaking the average in (30b) so that $\boldsymbol{\phi}(\mathbf{k},s)$ reads as

$$\mathbf{k}\cdot\boldsymbol{\phi}(\mathbf{k},s)\mathbf{k} \approx -\sigma^2 \int_{\mathbf{k}'} \mathbf{k}\cdot\tilde{\mathbf{C}}(\mathbf{k}')\mathbf{k}\overline{\tilde{c}^{*}}(\mathbf{k}-\mathbf{k}',s) \equiv$$

(41)

It is obtained diagrammatically by replacing the single line in the second-order loop diagram in (39) by a bold line and disregarding the other diagrams. Note that this one-loop closure approximation renders $\boldsymbol{\phi}(\mathbf{k},s)$ irreducible, i.e., consisting only of irreducible diagrams. According to (40), the generalized diffusivity is now consistently given by

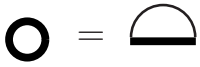

(42)

The self-consistency condition requires that only the first term on the right of (40) contributes to the generalized diffusivity as the remaining terms are reducible in the DIA closure approximation.

The DIA constitutes a one-loop closure, which is sometimes referred to as Corrsin's conjecture (e.g., [26,33,49]). It is equivalent to the Hartree-Fock approximation (e.g., [62]). In the context of perturbation approximations to the solution of the Kadar-Parisi-Zhang equation, this closure is called fastest apparent convergency [63]. For transport in random media, the scheme is called Gaussian closure (e.g., [15]). Mazzino [44] presents the renormalized perturbation theory leading to the DIA and the resulting two-point closure for the macrodispersion coefficients. Classical renormalization group studies analyzing the properties of randomly stirred

fluids routinely employ such one-loop resummation schemes (e.g., [45–47]).

The resulting effective transport equation for the Fourier Laplace transform of the Green's function is obtained by inserting Eq. (42) for the generalized diffusivity into Eq. (18),

$$s\overline{\tilde{c}^*}(\mathbf{k},s) - ik_1\overline{\tilde{c}^*}(\mathbf{k},s) + \mathbf{k}\cdot\mathbf{D}^m\mathbf{k}\overline{\tilde{c}^*}(\mathbf{k},s) + \sigma^2\int_{\mathbf{k}'}\mathbf{k}\cdot\tilde{\mathbf{C}}(\mathbf{k}')\mathbf{k}\overline{\tilde{c}^*}(\mathbf{k}-\mathbf{k}',s)\overline{\tilde{c}^*}(\mathbf{k},s). \tag{43}$$

The latter was first derived by Roberts [40]. The diagrammatic representation of the corresponding integral equation is given by

(44)

The DIA is a resummation scheme for the generalized diffusivity $\Sigma(\mathbf{k},s)$. The class of diagrams that are summed up can be determined by iterating the (nonlinear) integral Eq. (44) and substituting the result into the self-consistent closure (42). Up to sixth order, this procedure leads to

(45)

The scheme sums up the loop diagrams at any order, but disregards all cross diagrams. By construction, there is no double counting of diagrams. Recall that the cancellation of the cross and loop diagrams yields a zero transverse dispersion coefficient in $d=2$ dimensions. Thus, as we see in the following, the DIA leads to erroneous predictions in $d=2$.

According to Eq. (33), the asymptotic behavior of the macrodispersion coefficients predicted with the DIA closure is

$$D_{ij}^a = \sigma^2\int_{\mathbf{k}'}\tilde{C}_{ij}(\mathbf{k}')\overline{\tilde{c}^*}(-\mathbf{k}',0). \tag{46}$$

Combining Eq. (46) and (17) yields a well-known nonlinear system of equations for the macrodispersion coefficients (e.g., [26,41,42]),

$$D_{ij}^a = \sigma^2\int_{\mathbf{k}'}\frac{\tilde{C}_{ij}(\mathbf{k}')}{ik_1' + \mathbf{k}'\cdot(\mathbf{D}^m+\mathbf{D}^a)\mathbf{k}'}. \tag{47}$$

To solve Eq. (47) for arbitrary σ^2, we reduce the d-dimensional integrals to one-dimensional integrals analytically and solve the resulting equations numerically by employing the Newton method and evaluating the integrals with Gaussian quadratures. For the sake of simplicity, here and in the following, we employ the d-dimensional Kraichnan correlation model [2] with correlation length l,

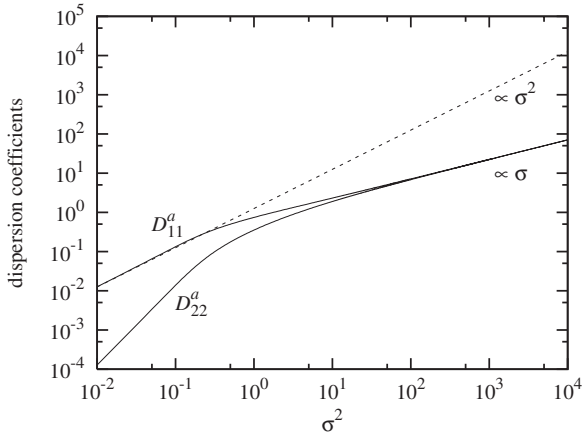

FIG. 1. Longitudinal and transverse asymptotic dispersion coefficients given by the two-point closure. The dashed line shows the second-order perturbation solution (27) for the longitudinal dispersion coefficient.

$$\tilde{C}_{ij}(\mathbf{x}) = \left(\delta_{ij} - \frac{k_i k_j}{k^2}\right)(2\pi)^{d/2}k^2\exp\left(-\frac{k^2}{2}\right)\exp(-i\mathbf{k}\cdot\mathbf{x}). \tag{48}$$

Figure 1 shows the corresponding solutions for the asymptotic longitudinal and transverse macrodispersion coefficients. For $\sigma^2 \ll 1$, it follows from Eq. (47) that

$$D_{11}^a \propto \sigma^2, \quad D_{ii}^a \propto \sigma^4, \quad i \neq 1, \tag{49}$$

i.e., the longitudinal coefficient is of order σ^2 and the transverse coefficients are of order σ^4. The former is consistent with the perturbation theory, while the latter is not. For large $\sigma^2 \gg 1$, a scaling argument (e.g., [42]) shows that the macrodispersion coefficient in Eq. (47) scales as

$$D_{ii}^a \propto \sigma, \quad \forall \quad i. \tag{50}$$

Thus, Corrsin's conjecture is not consistent with the exact solution (see [1] and Sec. III), according to which $D_{22}^a = 0$ in $d=2$ dimensions.

B. Four-point closure

To overcome the apparent inconsistency of Corrsin's conjecture, we develop a resummation scheme that takes into account cross diagrams and is exact for the transverse dispersion coefficient in $d=2$ spatial dimensions. Using the statistical homogeneity of the random flow field $\mathbf{u}'(\mathbf{x})$, we show in Appendix C that $\boldsymbol{\phi}(\mathbf{k},s)$ in Eq. (30b) can be expressed as

$$\boldsymbol{\phi}(\mathbf{k},s) = \boldsymbol{\phi}^{(2)}(\mathbf{k},s) + \prod_{i=1}^{4} \int_{\mathbf{k}^{(i)}} \tilde{c}_0^*(\mathbf{k}+\mathbf{k}^{(1)},s)\tilde{c}_0^*(\mathbf{k}-\mathbf{k}^{(4)},s) \times \overline{\tilde{c}^*(\mathbf{k}-\mathbf{k}^{(3)}-\mathbf{k}^{(4)},s)\tilde{\mathbf{u}}'(\mathbf{k}^{(1)}) \otimes \tilde{\mathbf{u}}'(\mathbf{k}^{(4)})(\mathbf{k}+\mathbf{k}^{(1)}) \cdot \tilde{\mathbf{u}}'(\mathbf{k}^{(2)})(\mathbf{k}-\mathbf{k}^{(4)}) \cdot \tilde{\mathbf{u}}'(\mathbf{k}^{(3)})}, \tag{51a}$$

where

$$\boldsymbol{\phi}^{(2)}(\mathbf{k},s) = -\sigma^2 \int_{\mathbf{k}'} \tilde{\mathbf{C}}(\mathbf{k}')\tilde{c}_0^*(\mathbf{k}-\mathbf{k}',s) \equiv \tag{51b}$$

As in the DIA, we break the average after the full propagator and evaluate the average over the random velocity field according to Wick's theorem, which yields

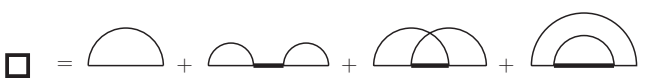

(52)

Diagrammatically this closure is performed by replacing the single lines in the center of the fourth-order diagrams in (39) with the bold lines, and disregarding the remaining higher-order diagrams.

Substituting (52) into (40) and retaining only the irreducible terms leads to a self-self-consistent expression for the generalized diffusivity $\tilde{\Sigma}(\mathbf{k},s)$,

(53)

Again here the self-consistency condition is imposed by the fact that the generalized diffusivity consists exclusively of irreducible contributions. The scheme is by construction exact up to fourth order. It also reproduces the exact result for the transverse dispersion in $d=2$ dimensions.

The corresponding (nonlinear) effective transport equation for the average propagator is now given by

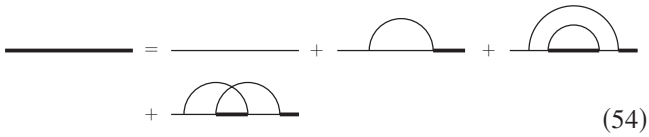

(54)

The class of diagrams accounted for by the four-point closure can be determined by iterating (54) and substituting the resulting series into the self-consistent expression (53). Thus, we obtain for the generalized diffusivity $\tilde{\Sigma}(\mathbf{k},s)$ up to sixth order

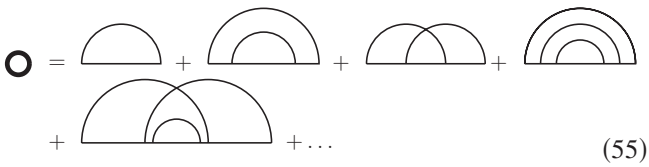

(55)

It is important to recognize the differences between the four-point closure (55) and the DIA closure (42). The four-point closure sums up systematically the cross and loop contributions of higher order, as illustrated in (55). It disregards the loop diagrams similar to the fourth diagram on the right-hand side of (42), which are accounted for by the DIA, but takes into account the cross diagrams similar to the fifth diagram in (55). Again as in the DIA, by construction there is no double counting of diagrams.

Substituting (53) into (14) and taking the limit as $s \to 0$ leads to an expression for the asymptotic dispersion coefficients,

$$D_{ij}^a = \delta^{(2)}D_{ij}^a + \delta^{(l)}D_{ij}^a + \delta^{(c)}D_{ij}^a, \tag{56a}$$

where $\delta^{(2)}D_{ij}^a$ is the long-time limit of (26), and $\delta^{(l)}D_{ij}^a$ and $\delta^{(c)}D_{ij}^a$ correspond to the loop and cross diagrams in (53),

$$\delta^{(l)}D_{ij}^a = -\sigma^4 \int_{\mathbf{k}'} \int_{\mathbf{k}''} \tilde{c}_0^*(-\mathbf{k}',0)^2 \tilde{C}_{ij}(\mathbf{k}')k_m' \tilde{C}_{ml}(\mathbf{k}'') \times k_l' \overline{\tilde{c}^*}(-\mathbf{k}'-\mathbf{k}'',0), \tag{56b}$$

$$\delta^{(c)}D_{ij}^a = -\sigma^4 \int_{\mathbf{k}'} \int_{\mathbf{k}''} \tilde{c}_0^*(-\mathbf{k}',0)\tilde{c}_0^*(-\mathbf{k}'',0)\tilde{C}_{il}(\mathbf{k}') \times k_l'' k_m' \tilde{C}_{mj}(\mathbf{k}'') \overline{\tilde{c}^*}(-\mathbf{k}'-\mathbf{k}'',0). \tag{56c}$$

Relations Eq. (55), along with Eq. (17) for the average concentration, constitute a nonlinear system of equations for the asymptotic macrodispersion coefficients.

1. Analytical solutions in two dimensions

In $d=2$ dimensions, the asymptotic limit of $\mathbf{D}^m \ll 1$ leads to the cancellation of the contributions to the transverse dispersion coefficient due to the loop and cross diagrams in Eq. (53), i.e.,

$$\lim_{\mathbf{D}^m \to \mathbf{0}} (\delta^{(l)}D_{ij}^a + \delta^{(c)}D_{ij}^a) = 0. \tag{57}$$

Since the second-order contribution $\delta_0^{(2)}\{\phi_{22}(\mathbf{0},s)\}=0$ in this limit, this gives

$$\lim_{\mathbf{D}^m \to \mathbf{0}} D_{22}^a \equiv 0. \tag{58}$$

This result is consistent with the exact result for the transverse dispersion coefficient, first derived in [1] (see also Sec. III), as it preserves the cancellation mechanism in accounting for the loop and cross contributions.

We show in Appendix D that combining Eq. (56) with the asymptotic average concentration Eq. (17) gives the follow-

ing nonlinear equation for the asymptotic longitudinal macrodispersion coefficient D_{11}^a:

$$D_{11}^a = \sigma^2\alpha_0 + \sigma^4 A_1(D_{11}^a) + \sigma^4 A_2(D_{11}^a), \tag{59a}$$

where α_0 is given by

$$\alpha_0 = \int_{\mathbf{k}'} \int_0^\infty d\mu\, \tilde{C}_{11}(\mathbf{k}')\exp(-i\mu k_1') \tag{59b}$$

and

$$A_1(D_{11}^a) = -\int_{\mathbf{k}'} \int_{\mathbf{k}''} \int_0^\infty d\mu\, \mu \int_0^\infty d\lambda \times \exp(-i\mu k_1') k_2'^2 \tilde{C}_{11}(\mathbf{k}')\tilde{C}_{22}(\mathbf{k}'') \times \exp[-\lambda D_{11}^a (k_1' + k_1'')^2 + i\lambda(k_1' + k_1'')], \tag{59c}$$

$$A_2(D_{11}^a) = 3\int_{\mathbf{k}'} \int_{\mathbf{k}''} \int_0^\infty d\lambda\, \tilde{C}_{11}(\mathbf{k}')\tilde{C}_{11}(\mathbf{k}'') \times \exp[-\lambda D_{11}^a (k_1' + k_1'')^2 + i\lambda(k_1' + k_1'')]. \tag{59d}$$

For arbitrary variances σ^2, the longitudinal macrodispersion coefficient D_{11}^a is obtained by solving the self-consistent equation (59) numerically, as outlined in Appendix D. For $\sigma^2 \gg 1$, the asymptotic behavior of D_{11}^a was determined analytically by noting that in the limit of large $D_{11}^a \gg 1$, both A_1 and A_2 behave as

$$A_i(D_{11}^a) = \alpha_i + \mathcal{O}\left(\frac{1}{D_{11}^a}\right), \quad i = 1,2, \tag{60a}$$

and

$$\alpha_0 = \sqrt{\frac{\pi}{2}}, \quad \alpha_1 = \alpha_2 = 3\sqrt{\pi}. \tag{60b}$$

Substituting Eq. (60) into Eq. (59), we obtain a new approximation for the longitudinal macrodispersion coefficient,

$$D_{11}^a = \alpha_0\sigma^2 + 2\alpha_1\sigma^4. \tag{61}$$

Recently, de Dreuzy *et al.* [30] reported such a dependence of the macroscopic asymptotic longitudinal dispersion coefficient, which they obtained from numerical random walk simulations in two-dimensional heterogeneous porous media. They also confirmed the lack of a disorder-induced contribution to lateral dispersion in the limit of small microdispersion.

2. Comparison to numerical simulations

Figure 2 compares the asymptotic longitudinal macrodispersion coefficients D_{11}^a obtained from the four-point and two-point closure schemes, fourth-order perturbation theory, and the results obtained from numerical random walk simulations of transport in the Gaussian random flow field characterized by the correlation function (48). The numerical simulations are described in Appendix E. It should be noted

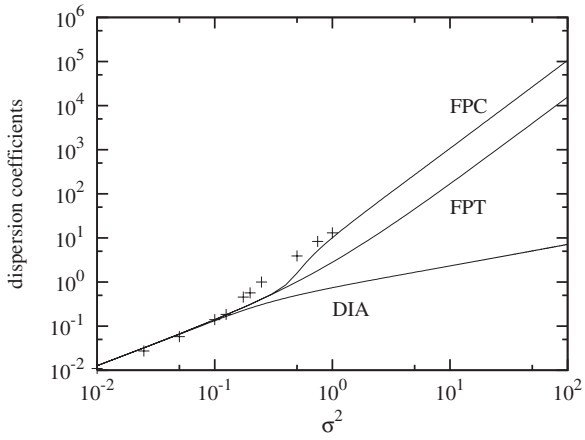

FIG. 2. Comparison of the longitudinal asymptotic dispersion coefficients as obtained from the DIA, the four-point closure scheme (FPC), fourth-order perturbation theory (FPT), and the numerical experiments (+).

that two-dimensional Gaussian random flow fields display closed streamlines as discussed, e.g., in [3,8,12]. As such, the limit of zero microdispersion leads to an anomalous increase of the longitudinal macrodispersion coefficient with time, $D_{11}(t) \propto t$, due to the trapping of particles in the closed streamlines and particle transport on open streamlines. However, in the presence of microdispersion, $D_{11}(t)$ converges to a constant asymptotic value D_{11}^a as t becomes large. Since the time required to reach this asymptote increases with the variance σ^2, we determine D_{11}^a only for a maximum variance of $\sigma^2 = 1$ due to limitations of computational resources. The presented results correspond to the local dispersion coefficients of $D_{11}^m \equiv D_{22}^m = 10^{-3}$; the correlation length l and mean flow velocity $\bar{u}$ are set to 1.

The numerical results presented in Fig. 2 conform with the fourth-order perturbation theory and the two- and four-point closures, as long as the variance remains small, $\sigma^2 \leq 10^{-1}$. This is to be expected since the system is perturbative for such small values, and all three schemes reduce to the second-order perturbation theory result (27).

For larger variances, the two-point closure significantly underestimates the numerical results. The macrodispersion coefficients given by the fourth-order perturbation theory underestimate the numerical findings but are more accurate than the two-point closure. Again, this should come as no surprise, since the cross terms that are disregarded by the two-point closure are taken into account. The four-point closure scheme underestimates the numerical results as well for $\sigma^2 \in [10^{-1}, 1]$, but performs better than perturbation theory and the two-point closure.

As σ^2 increases, the four-point closure yields macrodispersion values that are consistently larger than those obtained from the fourth-order perturbation theory and the two-point closure. The two-point closure yields macrodispersion values that are much smaller than those obtained from both alternative schemes.

Though somewhat limited because of the pathology of closed streamlines in two dimensions, this comparison shows that the cross-terms, which are disregarded in the two-point closure, need to be taken into account for a realistic quanti-

tative prediction of macrodispersion in incompressible static random flow fields. Furthermore, as pointed out above, the recent paper by de Dreuzy *et al.* [30] confirms the behavior obtained from the four-point closure scheme and demonstrates the failures and limitations of the DIA in predicting transport in strongly heterogeneous porous media.

V. SUMMARY AND CONCLUSIONS

We study transport in a static incompressible random flow field. Focusing on the impact of spatial fluctuations on the asymptotic macroscopic spreading of a passive scalar, we investigated the behavior of the macrodispersion coefficients (1). The latter has been the subject of intense research in the last three decades in the context of transport in random media and in particular for the quantification of contaminant spreading in heterogeneous aquifers. Mostly limited to perturbation theory analyses, many studies are strictly valid only for small or moderate fluctuations of the random flow field.

Most resummation schemes based on renormalization theory and self-consistent closures that are employed to overcome these limitations use so-called two-point closures (resulting in one-loop resummation schemes for the macrodispersion coefficients). These schemes are based on second-order expressions (in the fluctuations of the random velocity field). While such approaches perform very well for random velocities that are δ correlated in time, they are insufficient in the opposite limit of steady velocity fields. Specifically, they prove to be inconsistent for the quantification of transverse spreading in two spatial dimensions. We point out that this inconsistency is due to the fact that classical two-point schemes do not take into account a certain class of contributions (so-called cross contributions) to the perturbation series, which arise only in fourth order. To overcome this shortcoming, we derive a four-point closure for the ensemble average concentration of a solute, which yields the macrodispersion coefficients accounting for these critical contributions.

Classical field theory yields an exact though formal macroscopic evolution equation for the ensemble-averaged concentration distribution in terms of the generalized diffusivity (self-energy) $\Sigma(\mathbf{k},s)$ that encapsulates the impact of spatial heterogeneity on the macroscopic transport behavior. Using the translation invariance of the underlying random flow field we obtain expression (31) for the generalized diffusivity, which forms the basis for the derivation of the four-point closure and can be used straightforwardly to establish higher-order closure schemes.

Going beyond the lowest-order perturbation theory, we analyze the DIA scheme and similar two-point closure schemes. The expressions for the macrodispersion coefficients resulting from these approaches take into account contributions of all orders in the disorder variance but disregard a class of so-called cross terms. These terms arise at fourth order and thus are beyond the reach of classical one-loop schemes (which are based on second order). However, it is precisely this class of terms that plays a critical role for the quantification of transverse spreading in two spatial dimensions.

We derive and implement a four-point closure, which is exact for transverse dispersion in two dimensions. The resulting resummation scheme is evaluated for the macrodispersion coefficients in two spatial dimensions. It yields zero transverse dispersion, while the longitudinal macrodispersion coefficients increases monotonically with disorder variance. For strong fluctuations of the random flow field, the longitudinal macrodispersion coefficient increases as the square of the disorder variance as given by expression (61). These results are consistent with recently published Monte Carlo simulations [30] and the simulations presented in the paper. The DIA, in contrast, predicts an increase of the longitudinal and transverse macrodispersion coefficients with the square root of the disorder variance. A comparison of the four-point closure, fourth-order perturbation theory, and the DIA shows that the latter performs worst of the three closure schemes under consideration. The two-point DIA scheme is insufficient for the quantification of asymptotic solute spreading in biased incompressible random flow fields. Higher-order closure schemes, such as the one suggested in the present paper, are required to make reliable predictions for the disorder-induced spreading in random environments.

ACKNOWLEDGMENTS

M.D. acknowledges the support of the program "Ramon y Cajal" of the Spanish Ministry of Education and Science (MEC), ENRESA, the European Union IP FUNMIG (Contract No. 516514) and the MEC project MODEST (Project No. CGL-2005-05171). The work of D.M.T. was supported by the DOE Office of Science Advanced Scientific Computing Research (ASCR) program in Applied Mathematical Sciences.

APPENDIX A: FOURIER AND LAPLACE TRANSFORM

Let us define Fourier (denoted by the tilde) and Laplace (denoted by the asterisk) forward and inverse transform pairs as

$$\tilde{c}(\mathbf{k},t) = \int d\mathbf{x}\, e^{i\mathbf{k}\cdot\mathbf{x}} c(\mathbf{x},t), \quad c(\mathbf{x},t) = \int_{\mathbf{k}} e^{-i\mathbf{k}\cdot\mathbf{x}} \tilde{c}(\mathbf{k},t) \tag{A1}$$

and

$$\tilde{c}^*(\mathbf{k},s) = \int_0^\infty dt\, e^{-st} \tilde{c}(\mathbf{k},t), \quad \tilde{c}(\mathbf{k},t) = \int_{\gamma-i\infty}^{\gamma+i\infty} ds\, e^{st} \tilde{c}^*(\mathbf{k},s), \tag{A2}$$

respectively. In the definition of the inverse Laplace transform (A2), γ is chosen so that singularities of $\tilde{g}^*(s)$ lie to the left of the line $(\gamma-i\infty, \gamma+i\infty)$ [64].

APPENDIX B: GREEN'S FUNCTION

We focus here on the properties of the Green's function as a consequence of the statistical homogeneity of the random

field $\mathbf{u}(\mathbf{x})$. Let us define the Green's function $g_L(\mathbf{x},t|\mathbf{x}')$ as a solution of

$$\frac{\partial g_L(\mathbf{x},t|\mathbf{x}')}{\partial t} + \boldsymbol{\nabla}\cdot[\mathbf{u}_L(\mathbf{x}) - \mathbf{D}^m\boldsymbol{\nabla}]g_L(\mathbf{x},t|\mathbf{x}') = 0, \quad \text{(B1)}$$

$$\mathbf{u}_L(\mathbf{x}) \equiv \mathbf{u}(\mathbf{x}+\mathbf{L})$$

subject to the initial condition $g_L(\mathbf{x},0|\mathbf{x}') = \delta(\mathbf{x}-\mathbf{x}')$. One can verify by inspection that this solution is given by

$$g_L(\mathbf{x},t|\mathbf{x}') = g(\mathbf{x}+\mathbf{L},t|\mathbf{x}'+\mathbf{L}), \quad \text{(B2)}$$

Due to the statistical homogeneity of $\mathbf{u}(\mathbf{x})$, the ensemble means of $g_L(\mathbf{x},t|\mathbf{x}')$ and $g(\mathbf{x},t|\mathbf{x}')$ are identical. It then follows from Eq. (B2) that for an arbitrary $\mathbf{L}$

$$\bar{g}(\mathbf{x},t|\mathbf{x}') = \bar{g}(\mathbf{x}+\mathbf{L},t|\mathbf{x}'+\mathbf{L}). \quad \text{(B3)}$$

Setting $\mathbf{L}=-\mathbf{x}'$ in Eq. (B3) yields $\bar{g}(\mathbf{x},t|\mathbf{x}') = \bar{g}(\mathbf{x}-\mathbf{x}',t|\mathbf{0})$. Recalling Eq. (5), we obtain Eq. (9).

The stationarity of the random flow field also implies that functionals of $g(\mathbf{x},t|\mathbf{x}')$ and $\mathbf{u}(\mathbf{x})$ are translation invariant,

$$\begin{aligned}\overline{F[\{g(\mathbf{x},t|\mathbf{x}')\},\{\mathbf{u}'(\mathbf{x})\}]} &= \overline{F[\{g_L(\mathbf{x},t|\mathbf{x}')\},\{\mathbf{u}_L'(\mathbf{x})\}]} \\ &= \overline{F[\{g(\mathbf{x}+\mathbf{L}),t|\mathbf{x}'+\mathbf{L})\},\{\mathbf{u}'(\mathbf{x}+\mathbf{L})\}]}, \quad \text{(B4)}\end{aligned}$$

where we used Eq. (B2). Thus, we obtain for the three-point cross moments

$$\overline{u_i'(\mathbf{x}')g(\mathbf{x}'',t|\mathbf{y})} = \varphi_i^{(3)}(\mathbf{x}'-\mathbf{x}'',\mathbf{x}''-\mathbf{y},t), \quad \text{(B5)}$$

which in Fourier space reads as

$$\overline{\tilde{u}_i(\mathbf{k}')\tilde{g}(\mathbf{k}'',t|\mathbf{q})} = (2\pi)^d\tilde{\varphi}_i^{(3)}(\mathbf{k}',\mathbf{q},t)\delta(\mathbf{k}'+\mathbf{k}''+\mathbf{q}). \quad \text{(B6)}$$

For the four-point cross moments, we obtain accordingly

$$\overline{u_i'(\mathbf{x}')u_j'(\mathbf{x}'')g(\mathbf{x}''',t|\mathbf{y})} = \varphi_{ij}^{(4)}(\mathbf{x}'-\mathbf{x}'',\mathbf{x}''-\mathbf{x}''',\mathbf{x}'''-\mathbf{y},t), \quad \text{(B7)}$$

for which we obtain in Fourier space

$$\overline{\tilde{u}_i(\mathbf{k}')\tilde{u}_j(\mathbf{k}'')\tilde{g}(\mathbf{k}''',t|\mathbf{q})} = (2\pi)^d\tilde{\varphi}_{ij}^{(4)}(\mathbf{k}',\mathbf{k}'+\mathbf{k}'',\mathbf{q},t) \times\delta(\mathbf{k}'+\mathbf{k}''+\mathbf{k}'''+\mathbf{q}). \quad \text{(B8)}$$

APPENDIX C: ENSEMBLE AVERAGES

Relation (5) between the scalar field and the Green's function reads in Fourier-Laplace space as

$$\tilde{\bar{c}}^*(\mathbf{k},s) = \int_{\mathbf{q}}\tilde{\bar{g}}^*(\mathbf{k},s|\mathbf{q}). \quad \text{(C1)}$$

Using the translation invariance of the average Green's function as derived in the previous section, we obtain for $\tilde{\bar{c}}^*(\mathbf{k},s)$ in Fourier-Laplace space

$$\tilde{\bar{c}}^*(\mathbf{k},s) = \int_{\mathbf{q}}\tilde{\bar{g}}^*(\mathbf{k},s|\mathbf{q}) = \int_{\mathbf{q}}\tilde{\bar{g}}^*(-\mathbf{q},s|-\mathbf{k}), \quad \text{(C2)}$$

where $\tilde{g}^*(\mathbf{q},s|\mathbf{k})$ is the adjoint Green's function. The integral equation for the adjoint Green's function reads as

$$\tilde{g}^*(\mathbf{q},s|\mathbf{k}) = (2\pi)^d\delta(\mathbf{k}+\mathbf{q})\tilde{c}_0^*(-\mathbf{k},s) - \tilde{c}_0^*(-\mathbf{k},s) \times\int_{\mathbf{k}'} i\mathbf{k}\cdot\tilde{\mathbf{u}}'(\mathbf{k}')\tilde{g}^*(\mathbf{q},s|\mathbf{k}-\mathbf{k}'). \quad \text{(C3)}$$

In order to derive Eq. (30a) with Eq. (30b), we use (C3) in (C2), which yields

$$\tilde{\bar{c}}^*(\mathbf{k},s) = \tilde{c}_0^*(\mathbf{k},s) + \tilde{c}_0^*(\mathbf{k},s)\int_{\mathbf{k}'}\int_{\mathbf{q}} i\mathbf{k}\cdot\overline{\tilde{\mathbf{u}}'(\mathbf{k}')\tilde{g}^*(-\mathbf{q},s|-\mathbf{k}-\mathbf{k}')}. \quad \text{(C4)}$$

From Eq. (B6), we conclude that

$$\overline{\tilde{u}_i'(\mathbf{k}')\tilde{g}^*(-\mathbf{q},s|-\mathbf{k}-\mathbf{k}')} = \overline{\tilde{u}_i'(\mathbf{k}')\tilde{g}^*(\mathbf{k},s|\mathbf{q}-\mathbf{k}')}, \quad \text{(C5)}$$

so that Eq. (C4) can be written as

$$\tilde{\bar{c}}^*(\mathbf{k},s) = \tilde{c}_0^*(\mathbf{k},s) + \tilde{c}_0^*(\mathbf{k},s)\int_{\mathbf{k}'}\int_{\mathbf{q}} i\mathbf{k}\cdot\overline{\tilde{\mathbf{u}}'(\mathbf{k}')\tilde{g}^*(\mathbf{k},s|\mathbf{q})}, \quad \text{(C6)}$$

where we shifted $\mathbf{q}\to\mathbf{q}+\mathbf{k}'$. Using Eq. (C1) gives

$$\tilde{\bar{c}}^*(\mathbf{k},s) = \tilde{c}_0^*(\mathbf{k},s) + \tilde{c}_0^*(\mathbf{k},s)\int_{\mathbf{k}'} i\mathbf{k}\cdot\overline{\tilde{\mathbf{u}}'(\mathbf{k}')\tilde{c}^*(\mathbf{k},s)}. \quad \text{(C7)}$$

Substituting the right side of Eq. (10) into the right side of Eq. (C7) gives Eq. (30a) with (30b).

For the derivation of Eq. (51), we iterate the integral equation Eq. (C3) once and insert the right side of the resulting equation into the right side of Eq. (C2). This yields

$$\tilde{\bar{c}}^*(\mathbf{k},s) = \tilde{c}_0^*(\mathbf{k},s) - \tilde{c}_0^*(\mathbf{k},s)\int_{\mathbf{k}'}\int_{\mathbf{k}''}\int_{\mathbf{q}}\tilde{c}_0^*(\mathbf{k}+\mathbf{k}',s) \times\mathbf{k}\cdot\overline{\tilde{\mathbf{u}}'(\mathbf{k}')(\mathbf{k}+\mathbf{k}')\cdot\tilde{\mathbf{u}}'(\mathbf{k}'')\tilde{g}^*(-\mathbf{q},s|-\mathbf{k}-\mathbf{k}'-\mathbf{k}'')}. \quad \text{(C8)}$$

With the same arguments as above, we obtain by using relation Eq. (B8)

$$\tilde{\bar{c}}^*(\mathbf{k},s) = \tilde{c}_0^*(\mathbf{k},s) - \tilde{c}_0^*(\mathbf{k},s)\int_{\mathbf{k}'}\int_{\mathbf{k}''}\tilde{c}_0^*(\mathbf{k}+\mathbf{k}',s) \times\mathbf{k}\cdot\overline{\tilde{\mathbf{u}}'(\mathbf{k}')(\mathbf{k}+\mathbf{k}')\cdot\tilde{\mathbf{u}}'(\mathbf{k}'')\tilde{c}^*(\mathbf{k},s)}. \quad \text{(C9)}$$

Iterating (10) once and substituting the right side of the resulting integral equation into (C9) gives (30) with (51).

APPENDIX D: INTEGRALS

Inserting Eq. (17) and (11) into Eq. (56b) and (56c) for $\mathbf{D}^m=\mathbf{0}$, we obtain

$$\delta D_{11}^{(c)} = 2\sigma^4 \int_{\mathbf{k}'} \int_{\mathbf{k}''} \int_0^\infty d\lambda\ \tilde{C}_{11}(\mathbf{k}')\tilde{C}_{11}(\mathbf{k}'')\exp\{-\lambda[i(k_1' + k_1'') + D_{11}^a(k_1' + k_1'')^2]\}, \tag{D1}$$

$$\delta D_{11}^{(l)} = \frac{1}{2}\delta D_{11}^{(c)} - \sigma^4 \int_{\mathbf{k}'} \int_{\mathbf{k}''} \int_0^\infty d\mu\ \mu \int_0^\infty d\lambda \times \exp(-i\mu k_1')\tilde{C}_{11}(\mathbf{k}')k_2'^2\tilde{C}_{22}(\mathbf{k}'')\exp\{-\lambda[i(k_1' + k_1'') + D_{11}^a(k_1' + k_1'')^2]\}. \tag{D2}$$

$A_1(D_{11}^a)$ is defined by $A_1(D_{11}^a) = \delta D_{11}^{(l)} - 1/2\,\delta D_{11}^{(c)}$ and $A_2(D_{11}^a) = 3/2\,\delta D_{11}^{(c)}$.

Inserting Eq. (48) into Eq. (D1) and (D2), we obtain for $A_1(D_{11}^a)$ and $A_2(D_{11}^a)$

$$A_1(D_{11}^a) = 3\int_0^\infty d\lambda \int_0^\infty d\mu\ \mu \times \exp\left(-\frac{2\lambda^2 + 2\mu^2 D_{11}^a \lambda + 2\mu\lambda + \mu^2}{2(1 + 4D_{11}^a\lambda)}\right) \times \frac{\lambda^2 - 4\mu\lambda^2 D_{11}^a + 4\lambda^2\mu^2 D_{11}^{a2} - 8\lambda^2 D_{11}^{a2} - 6D_{11}^a\lambda - 1}{(4D_{11}^a\lambda + 1)^{5/2}}, \tag{D3}$$

$$A_2(D_{11}^a) = \frac{3\sqrt{\pi}}{2}\left[1 + \exp\left(\frac{1}{4D_{11}^{a2}}\right)\mathrm{erfc}\left(\frac{1}{D_{11}^a}\right)\right]. \tag{D4}$$

The self-consistent equation (59) is solved using the Newton method (e.g., [65]), the double integral in (D3) is solved numerically using Gaussian quadratures. In the limit of $D_{11}^a \gg 1$, the above expressions can be solved analytically and give (59).

APPENDIX E: NUMERICAL SIMULATIONS

One realization of the random flow field $\mathbf{u}(\mathbf{x})$ is generated as a superposition of randomly chosen harmonic modes (e.g., [2–4,12]),

$$u_i(\mathbf{x}) = \bar{u}\delta_{i1} + \sigma\bar{u}\sqrt{\frac{2}{N}}\sum_{j=1}^{N} p_i(\mathbf{k}^{(j)})\cos(\mathbf{k}^{(j)}\cdot\mathbf{x} + \varphi^{(j)}). \tag{E1}$$

The vectors $\mathbf{k}^{(j)}$ and the phases $\varphi^{(j)}$ are independent random numbers. The wave vectors $\mathbf{k}^{(j)}$ are drawn from a two-dimensional Gaussian distribution with vanishing average and variance $1/l^2$. The phases $\varphi^{(j)}$ are equally distributed in the interval $[0, 2\pi]$. Here we used $N = 100$ modes.

The Langevin equation that is associated with the Fokker-Planck equation (2) is given by (e.g., [66])

$$\frac{\mathrm{d}}{\mathrm{d}t}\mathbf{x}(t) = \mathbf{u}(\mathbf{x}(t)) + \boldsymbol{\xi}(t), \tag{E2}$$

where $\boldsymbol{\xi}(t)$ represents a two-dimensional Gaussian white noise defined by $\langle\xi_i(t)\rangle = 0$ and $\langle\xi_i(t)\xi_j(t')\rangle = 2D\delta_{ij}\delta(t-t')$. The angular brackets denote the average over all white noise realizations. The macrodispersion coefficients then are given by

$$D_{ij}(t) = 1/2\frac{d}{dt}\{\overline{\langle x_i(t)x_i(t)\rangle} - \overline{\langle x_i(t)\rangle\langle x_i(t)\rangle}\}. \tag{E3}$$

The Langevin equation (E2) is solved using the extended Runge-Kutta method given in [4] instead of the common Euler method which follows from a straightforward time discretization of Eq. (E2). The accuracy of the extended Runge-Kutta scheme used here for the calculation of the particle path lines is of the order $\Delta t^{3/2}$, whereas the Euler method provides an accuracy of order $\Delta t^{1/2}$ only. The simulations were performed for 1000 realizations of the random flow field $\mathbf{u}(\mathbf{x})$, ten realizations of the white noise in each realization of $\mathbf{u}(\mathbf{x})$ and a time discretization of $\Delta t = 10^{-1}$.

[1] S. Attinger, M. Dentz, and W. Kinzelbach, Stochastic Environ. Res. Risk Assess. **18**, 9 (2004).
[2] R. H. Kraichnan, J. Fluid Mech. **13**, 22 (1970).
[3] R. H. Kraichnan, J. Fluid Mech. **77**, 753 (1976).
[4] I. T. Drummond, S. Duane, and R. R. Horgan, J. Fluid Mech. **138**, 75 (1984).
[5] W. D. McComb, *The Physics of Fluid Turbulence* (Clarendon Press, New York, 1991).
[6] U. Frisch, *Turbulence* (Cambridge University Press, Cambridge, U.K., 1995).
[7] J. P. Bouchaud and A. Georges, Phys. Rep. **195**, 127 (1990).
[8] M. B. Isichenko, Rev. Mod. Phys. **64**, 961 (1992).
[9] P. K. Kitanidis, J. Hydrol. **102**, 453 (1988).
[10] U. Jaekel and H. Vereecken, Water Resour. Res. **33**, 2287 (1997).
[11] H. Schwarze, U. Jaeckel, and H. Vereecken, Transp. Porous Media **43**, 265 (2001).
[12] M. Dentz, H. Kinzelbach, S. Attinger, and W. Kinzelbach, Water Resour. Res. **38**, 1118 (2002).
[13] J. A. Aronovitz and D. R. Nelson, Phys. Rev. A **30**, 1948 (1984).
[14] D. S. Fisher, D. Friedan, Z. Qiu, S. J. Shenker, and S. H. Shenker, Phys. Rev. A **31**, 3841 (1985).
[15] M. W. Deem, Phys. Rev. E **51**, 4319 (1995).
[16] D. S. Dean, I. T. Drummond, and R. R. Horgan, Phys. Rev. E **63**, 061205 (2001).
[17] T. Komorowski and S. Olla, J. Stat. Phys. **108**, 647 (2002).
[18] Y. Rubin, Water Resour. Res. **26**, 133 (1990).
[19] V. Kapoor and P. K. Kitanidis, Transp. Porous Media **22**, 91 (1996).
[20] D. McLaughlin and F. Ruan, Transp. Porous Media **42**, 133 (2001).
[21] M. Dentz, H. Kinzelbach, S. Attinger, and W. Kinzelbach, Phys. Rev. E **67**, 046306 (2003).

[22] G. Dagan, *Flow and Transport in Porous Formations* (Springer, New York, 1989).
[23] Y. Rubin, *Applied Stochastic Hydrogeology* (Oxford University Press, New York, 2003).
[24] L. W. Gelhar and C. L. Axness, Water Resour. Res. **19**, 161 (1983).
[25] G. Dagan, J. Fluid Mech. **145**, 151 (1984).
[26] G. Dagan, Water Resour. Res. **30**, 2699 (1994).
[27] K. Hsu, D. Zhang, and S. P. Neuman, Water Resour. Res. **32**, 571 (1996).
[28] B. X. Hu, A. E. Hassan, and J. H. Cushman, Water Resour. Res. **35**, 3685 (1999).
[29] B. X. Hu, H. Huang, A. E. Hassan, and J. H. Cushman, Adv. Water Resour. **25**, 513 (2002).
[30] J.-R. De Dreuzy, A. Beaudoin, and J. Erhel, Water Resour. Res. **43**, W10439 (2007).
[31] M. Avellaneda and A. J. Majda, Commun. Math. Phys. **131**, 381 (1990).
[32] D. L. Koch and E. S. G. Shaqfeh, Phys. Fluids A **4**, 887 (1992).
[33] Q. Zhang, Adv. Water Resour. **20**, 317 (1997).
[34] A. J. Majda and P. R. Kramer, Phys. Rep. **314**, 237 (1999).
[35] A. Mazzino, S. Musacchio, and A. Vulpiani, Phys. Rev. E **71**, 011113 (2005).
[36] R. Phythian and W. D. Curtis, J. Fluid Mech. **89**, 241 (1978).
[37] M. Avellaneda and A. J. Majda, Commun. Math. Phys. **138**, 339 (1991).
[38] J. L. Auriault and P. M. Adler, Adv. Water Resour. **18**, 217 (1995).
[39] R. H. Kraichnan, J. Fluid Mech. **5**, 497 (1959).
[40] P. H. Roberts, J. Fluid Mech. **11**, 257 (1961).
[41] S. P. Neuman and Y. Zhang, Water Resour. Res. **26**, 887 (1990).
[42] Q. Zhang, Water Resour. Res. **31**, 2955 (1995).
[43] P. R. Kramer, A. J. Majda, and E. Vanden-Eijnden, J. Stat. Phys. **111**, 565 (2003).
[44] A. Mazzino, Phys. Rev. E **56**, 5500 (1997).
[45] D. Forster, D. R. Nelson, and M. J. Stephen, Phys. Rev. A **16**, 732 (1977).
[46] C. De Dominicis and P. C. Martin, Phys. Rev. A **19**, 419 (1979).
[47] N. V. Antonov, Phys. Rev. E **60**, 6691 (1999).
[48] A. A. Abrikosov, L. P. Gorkov, and I. E. Dzyaloshinski, *Methods of Quantum Field Theory in Statistical Physics* (Courier Dover Publications, New York, 1975).
[49] R. H. Kraichnan, Complex Syst. **1**, 805 (1987).
[50] R. H. Kraichnan, Phys. Rev. **109**, 1407 (1958).
[51] D. L. Koch and J. F. Brady, J. Fluid Mech. **180**, 387 (1987).
[52] R. Zwanzig, *Lectures in Theoretical Physics* (Interscience Publishers, New York, 1961), Vol. III.
[53] R. Zwanzig, Phys. Rev. **124**, 983 (1961).
[54] I. T. Drummond and R. R. Horgan, J. Phys. A **20**, 4661 (1987).
[55] M. Sadovskii, *Diagrammatics* (World Scientific, Singapore, 2006).
[56] M. Dentz and B. Berkowitz, Phys. Rev. E **72**, 031110 (2005).
[57] S. P. Neuman, C. L. Winter, and C. M. Newman, Water Resour. Res. **23**, 453 (1987).
[58] P. McCarty and W. Horsthemke, Phys. Rev. A **37**, 2112 (1988).
[59] R. Mauri, Phys. Fluids A **3**, 743 (1991).
[60] R. Mauri, Phys. Fluids **7**, 275 (1995).
[61] I. Lunati, S. Attinger, and W. Kinzelbach, Water Resour. Res. **38**, 1187 (2002) .
[62] G. Parisi, *Statistical Field Theory* (Perseus Books, Massachusetts, 1998).
[63] T. Blum and A. J. Mc Kane, Phys. Rev. E **52**, 4741 (1995).
[64] H. S. Carslaw and J. C. Jaeger, *Conduction of Heat in Solids* (Oxford University Press, New York, 1959).
[65] W. H. Press, S. A. Teukolsky, W. T. Vetterling, and B. P. Flanner, *Numerical Recipes in C: The Art of Scientific Computing*, 2nd ed. (Cambridge Unversity Press, Cambridge, U.K., 2002).
[66] H. Risken, *The Fokker-Planck Equation* (Springer, Heidelberg, 1996).